

# Kondo temperature dependence of the Kondo splitting in a single-electron transistor

S. Amasha,<sup>1</sup> I. J. Gelfand,<sup>2</sup> M. A. Kastner,<sup>1,\*</sup> and A. Kogan<sup>1,†</sup>

<sup>1</sup>*Department of Physics, Massachusetts Institute of Technology, Cambridge, Massachusetts 02139*

<sup>2</sup>*Division of Engineering and Applied Sciences, Harvard University, Cambridge, Massachusetts 02138*

The Kondo peak in the differential conductance of a single-electron transistor is measured as a function of both magnetic field and the Kondo temperature. We observe that the Kondo splitting decreases logarithmically with Kondo temperature and that there exists a critical magnetic field  $B_C$  below which the Kondo peak does not split, in qualitative agreement with theory. However, we find that the magnitude of the prefactor of the logarithm is much larger than predicted and is independent of  $B$ , in contradiction with theory. Our measurements also indicate that the value of  $B_C$  is smaller than predicted.

PACS numbers: 73.23.Hk, 72.15.Qm, 75.20.Hr

The many-electron Kondo state is formed when conduction electrons screen a magnetic impurity. An important tool for studying the Kondo effect is the single-electron transistor (SET)<sup>1,2,3,4</sup> which consists of a confined droplet of electrons, called an artificial atom or a quantum dot, coupled by tunnel barriers to two conducting leads, called the source and the drain. When the quantum dot contains an odd number of electrons, and hence a net spin, the conduction electrons in the leads screen the spin on the dot and enhance the conductance of the SET. By using the gate electrodes that define the artificial atom to tune its parameters, Goldhaber-Gordon *et al.*<sup>5</sup> have tested the predictions of renormalization group calculations and scaling theory and have shown that the equilibrium properties of the SET are quantitatively described by the Anderson Hamiltonian.

SETs also provide the unique possibility of exploring non-equilibrium Kondo phenomena by applying a DC voltage  $V_{ds}$  between the drain and the source. A sensitive test<sup>6,7,8,9,10</sup> of theories of non-equilibrium Kondo physics is the measurement of the splitting in a magnetic field  $B$  of the Kondo peak in differential conductance as a function of  $V_{ds}$ . Calculations by Meir *et al.*<sup>6</sup> predict that in a magnetic field the Kondo peaks occur at  $eV_{ds} = \pm\Delta$ , where  $\Delta = |g|\mu_B B$  is the Zeeman energy for spin splitting and  $\mu_B = 58 \mu\text{eV/T}$  is the Bohr magneton. We define  $\Delta_K/e$  as half the separation in  $V_{ds}$  between the two peaks, so Meir *et al.* predict  $\Delta_K = \Delta$ . Early measurements by Cronenwett *et al.*<sup>4</sup> agree with this prediction. However calculations of spectral functions predict new features in the Kondo splitting. Costi<sup>7</sup> predicts that the screening of the spin on the quantum dot by the conduction electrons should cause the Kondo peak to split only above a critical magnetic field  $B_C$ , which depends on the Kondo temperature  $T_K$ , the energy scale that describes the strength of the screening. Moore and Wen<sup>8</sup> identify the field-induced splitting in their spectral function with the splitting in differential conductance and predict that the screening should cause  $\Delta_K < \Delta$  at all fields. Specifically, for  $1 < \Delta/k_B T_K < 100$  they predict that  $\Delta_K/\Delta$  increases logarithmically toward 1 as  $\Delta/k_B T_K$  increases. Recent observations by Kogan *et al.*<sup>11</sup> have confirmed the presence of the critical magnetic field  $B_C$ . However the

latter measurements, as well as those of Zumbühl *et al.*<sup>12</sup>, show that  $\Delta_K > \Delta$  at high fields, in disagreement with theory.

Here we extend the work of Kogan *et al.*<sup>11</sup> by reporting measurements of  $\Delta_K$  as a function of the Kondo temperature  $T_K$ , as well as  $B$ . These measurements exploit the property of SETs that  $T_K$  varies continuously with gate voltage, in contrast with conventional Kondo systems, for which  $T_K$  is determined by chemistry. We find  $\Delta_K > \Delta$  for high fields at the lowest Kondo temperatures, as observed previously. We also observe that  $\Delta_K$  decreases as  $\ln(T_{K,0}/T_K)$  with increasing  $T_K$ , where  $T_{K,0}$  is a constant. This logarithmic decrease in  $\Delta_K$  with increasing  $T_K$  qualitatively agrees with theory. However, theory predicts that the decrease should be proportional to  $|g|\mu_B B \ln(T_{K,0}/T_K)$ , whereas we find the prefactor of the logarithm to be much larger than predicted and independent of  $B$ . Our measurements also show that there is a critical magnetic field  $B_C$  for splitting the Kondo peak, as predicted. However, we find that the quantitative predictions for  $B_C$  as a function of  $T_K$  are not consistent with our data.

The SET we study is fabricated from a heterostructure consisting of an undoped GaAs buffer, followed by a 15 nm layer of  $\text{Al}_{0.3}\text{Ga}_{0.7}\text{As}$   $\delta$ -doped twice with a total of  $10^{13} \text{ cm}^{-2}$  of Si, and finally a 5 nm GaAs cap. The two-dimensional electron gas (2DEG) formed at the Al-GaAs/GaAs interface has an electron density of  $8.1 \times 10^{11} \text{ cm}^{-2}$  and a mobility of  $10^5 \text{ cm}^2/\text{Vs}$  at 4.2 K. Although the density of the 2DEG is high, magneto-transport measurements show that only a single subband is occupied. Electron-beam lithography is used to define the gate electrode pattern shown in the inset of Fig. 2(b). Applying a negative voltage to these electrodes depletes the 2DEG underneath them and forms an artificial atom of about 50 electrons isolated by two tunnel barriers from the remaining 2DEG regions, the source and drain leads. The electrochemical potential of the dot, as well as the coupling between the dot and the leads, can be tuned by changing the voltages on the electrodes. The voltage on the gate electrode  $g$  is denoted  $V_g$ . The SET is measured in a 75  $\mu\text{W}$  Oxford Instruments dilution refrigerator with an 8 T magnet and a lowest electron temperature of about

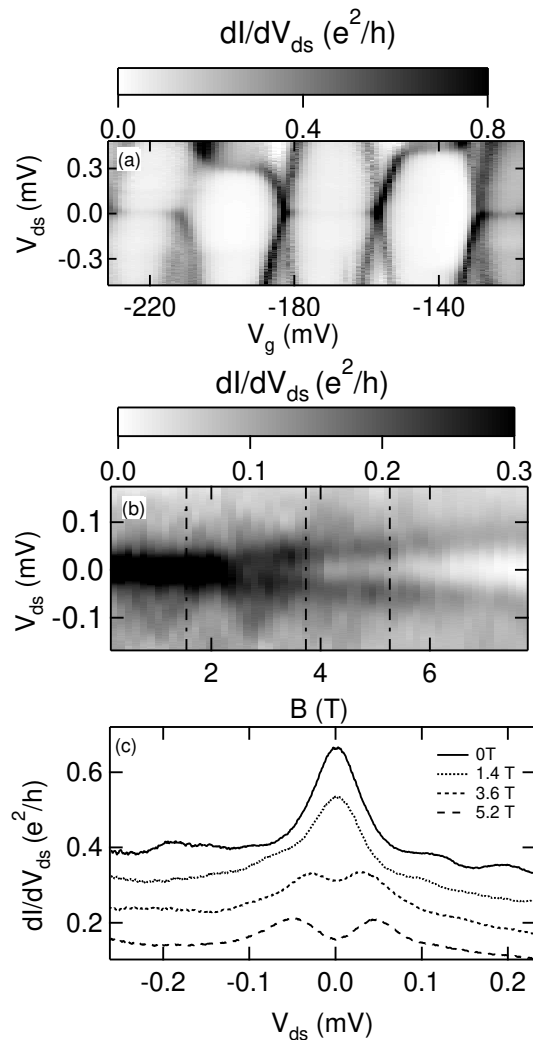


FIG. 1: (a) Coulomb blockade diamonds when the artificial atom is strongly coupled to the leads. The Kondo effect shows up as sharp resonances near  $V_{ds} = 0$  in the odd valleys. (b) Evolution of a Kondo peak as a function of magnetic field. Note that the splitting does not begin until  $B = 2.4$  T. These data are from a different experiment from those in (a). (c)  $dI/dV_{ds}$  vs  $V_{ds}$  for  $B = 0$  T and for other values of  $B$  marked by the dash-dot lines in (b). For  $B < 2.4$  T there is only one Kondo peak; above the threshold it splits. The traces have been offset by  $0.08 e^2/h$  for clarity.

100 mK. To minimize orbital effects we align the 2DEG parallel to the magnetic field to within a few degrees. We measure the differential conductance  $dI/dV_{ds}$  utilizing standard lock-in techniques. Careful measurements<sup>11</sup> of the  $g$ -factor of our SET using inelastic cotunneling and electron addition spectroscopy give  $|g| = 0.16$ .

We observe the Kondo effect by tuning the gate voltages so that the artificial atom is strongly coupled to the leads. Figure 1(a) shows an example of a plot of  $dI/dV_{ds}$  as a function of  $V_{ds}$  and  $V_g$ . Enhancements in the conductance at  $V_{ds} = 0$  in the middle of the Coulomb block-

ade valleys with an odd number of electrons are clearly visible. A sharp peak in  $dI/dV_{ds}$  as a function of  $V_{ds}$  in the middle of a Coulomb valley, where resonant tunneling is prohibited by energy and charge conservation, is the hallmark of the Kondo effect. An example of a peak at  $B = 0$  T is shown in Fig. 1(c). Applying a magnetic field causes the Kondo peak to split into two peaks above and below  $V_{ds} = 0$ . This is shown in Fig. 1(b), while Fig. 1(c) shows  $dI/dV_{ds}$  vs  $V_{ds}$  at various magnetic fields.

To study the splitting of a Kondo peak in  $dI/dV_{ds}$  as a function of  $T_K$ , we take advantage of the fact that  $T_K$  varies across a Coulomb valley. The dependence of  $T_K$  on the energy  $\epsilon_0$  of an unpaired electron in the artificial atom referenced to the Fermi level is given by<sup>5,13</sup>

$$T_K = \frac{\sqrt{\Gamma U}}{2k_B} \exp[\pi\epsilon_0(\epsilon_0 + U)/\Gamma U] \quad (1)$$

Here  $\Gamma$  is the full width at half-maximum of the Coulomb blockade peaks and  $U$  is the charging energy necessary to add an electron to the artificial atom. Goldhaber-Gordon *et al.*<sup>5</sup> have shown that their measurements of  $T_K$  are fit well by this equation. For our work, it is most convenient to re-write this equation in terms of the change in energy from the value in the middle of the Coulomb valley. We have

$$T_K = T_{K,0} \exp[\pi(\Delta\epsilon)^2/\Gamma U] \quad (2)$$

In this equation,  $T_{K,0}$  is the Kondo temperature in the middle of the Coulomb valley, and  $\Delta\epsilon$  is the difference in the energy from its value in the middle of the valley.  $\Delta\epsilon$  is related to the gate voltage by  $\Delta\epsilon = \alpha_g e(V_g - V_{g,0})$  where  $\alpha_g$  is the ratio of the gate capacitance to the total capacitance and  $V_{g,0}$  is the value of  $V_g$  in the middle of the valley. We can thus re-write the argument of the exponential in Equation (2) as  $\chi(V_g - V_{g,0})^2$  where  $\chi = \pi\alpha_g^2 e^2/\Gamma U$ . The Kondo temperature is a minimum in the middle of the Coulomb valley and increases exponentially close to the Coulomb blockade peaks. Thus, by varying  $V_g$ , we can study the variation in  $\Delta_K$  as a function of  $T_K$ . If the Kondo temperature gives a logarithmic correction to the splitting as predicted,<sup>8</sup> then we expect  $\Delta_K$  to vary quadratically in gate voltage.

To make quantitative comparisons with theory we need to know  $T_K$  throughout the Coulomb valley. To determine  $T_K$  we follow Goldhaber-Gordon *et al.*<sup>5</sup> and measure the differential conductance at  $V_{ds} = 0$  as a function of temperature. We then fit these data to an empirical form that gives a good approximation to numerical renormalization group results<sup>14</sup> to obtain the Kondo temperature  $T_K$ . This fit is accurate only if we have data for temperatures as low as  $T \sim 0.1T_K$ . The lowest temperature we can achieve is about 100 mK, so we can reliably measure Kondo temperatures larger than approximately 1 K. The Kondo temperature in the middle of the Coulomb blockade valley is significantly lower than this, so we cannot measure it directly. However, we can measure  $T_K$  near the Coulomb blockade peaks where the

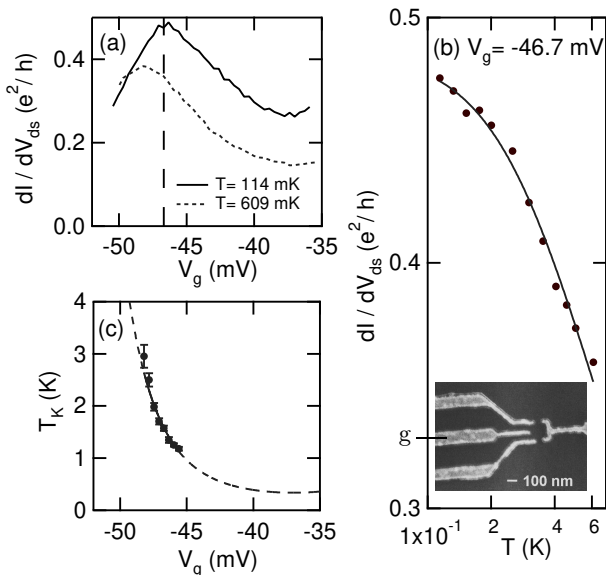


FIG. 2: (a)  $dI/dV_{ds}$  vs  $V_g$  at  $V_{ds} = 0$  for a Coulomb charging peak and half a Coulomb valley at two different temperatures. (b)  $dI/dV_{ds}$  as a function of temperature for the value of  $V_g$  marked by the dashed line in (a). Fitting these data gives  $T_K = 1.57 \pm 0.05$  K. The inset shows an electron micrograph of an SET similar to the one we studied. (c)  $T_K$  as a function of  $V_g$ . The solid line through the data points shows the result of fitting to Equation (2). The dashed curve is the extrapolation of Equation (2) using the results of the fit. Thus the fit allows us to estimate the Kondo temperature throughout the Kondo valley.

Kondo temperature is much higher. Fitting the latter data for  $T_K$  as a function of  $V_g$  to Equation (2) we can determine  $T_{K,0}$  and  $\chi$ , and then extrapolate to find the Kondo temperature throughout the valley.

Figure 2 illustrates this procedure. Figure 2(a) shows a Coulomb charging peak and half the Coulomb valley at two different temperatures. As the temperature is raised, the suppression of the Kondo effect removes the energy renormalization, causing the peak to move toward the bare resonance.<sup>5,15</sup> We measure  $dI/dV_{ds}$  at  $V_{ds} = 0$  as a function of temperature at several values of  $V_g$ , one of which is shown in Fig. 2(b), and fit these data to the empirical form<sup>5</sup> to determine  $T_K$ . Finally, Fig. 2(c) shows  $T_K$  as a function of  $V_g$  for the range in which it can be determined with confidence. Fitting these data to Equation (2) we find  $T_{K,0} = 340 \pm 30$  mK and  $\chi = 0.016 \pm 0.001$  (mV)<sup>-2</sup>. We can use our value of  $\chi$  to estimate  $\Gamma$ . From nearby Coulomb charging diamonds, we estimate  $U = 1.2$  mV and  $\alpha_g = 0.05$ . Combining this with our value of  $\chi$  we find that  $\Gamma \approx 420$   $\mu$ eV. Our values are similar to those obtained by Goldhaber-Gordon *et al.*,<sup>5</sup> who found  $U = 1.9 \pm 0.05$  meV,  $\alpha_g = 0.069 \pm 0.0015$ ,

and  $\Gamma = 280 \pm 10$   $\mu$ eV, and are consistent with having a somewhat larger artificial atom with stronger coupling to the leads. As expected for this stronger coupling,  $T_{K,0}$  in our SET is larger than that of Goldhaber-Gordon *et al.*<sup>5</sup>

To study the dependence of  $\Delta_K$  on  $T_K$  we measure  $dI/dV_{ds}$  as a function of  $V_{ds}$  and  $V_g$  at various magnetic fields. An example of such a measurement is shown in Fig. 3(a). We measure  $\Delta_K$  at each value of  $V_g$  by determining the separation in  $V_{ds}$  between the two peaks in  $dI/dV_{ds}$ ;  $\Delta_K$  is then half this value. The results for two different magnetic fields are shown in Fig. 3(b) and (c). The values of  $\Delta_K$  as a function of  $V_g$  are shown below the plots. These data are fit very well by parabolas, one of which is shown in Fig. 3(c). As discussed above, a parabola is what one would expect from a correction to  $\Delta_K$  that is logarithmic in the Kondo temperature.

One important feature of these data is that for  $B > 4$  T, the maxima of the the  $\Delta_K$  vs  $V_g$  curves lie above  $\Delta = |g|\mu_B B$ , where the value of  $\Delta$  is determined precisely using inelastic cotunneling.<sup>11</sup> By fitting  $\Delta_K(V_g)$  to a parabola, we extract the maximum value of  $\Delta_K$ , which is plotted as a function of magnetic field in Figure 4(a). The solid line shows the value of  $\Delta$  from cotunneling measurements. These data show that for large magnetic fields,  $\Delta_K > \Delta$  as observed previously.<sup>11,12</sup>

Another important feature of these data is the curvature of the parabolas, which is plotted versus  $B$  in Fig. 4(b). Moore and Wen<sup>8</sup> predict that for  $1 < \Delta/k_B T_K < 100$ ,  $\Delta_K/\Delta = b \ln(\Delta/k_B T_K) + constant$  where  $b$  is a constant of proportionality and is approximately 0.04. From Equation (2),  $T_K$  varies exponentially with gate voltage so that at fixed magnetic field the prediction is  $\Delta_K = \Delta_{K,0} - b(|g|\mu_B B)\chi(V_g - V_{g,0})^2$ , where  $\Delta_{K,0}$  gives the field splitting at the center of the valley. This is the equation of a parabola in  $V_g$  whose curvature becomes more negative with increasing magnetic field. This prediction is plotted in Fig. 4(b) and clearly does not agree with the data. The magnitude of the curvature is much larger than predicted by theory and does not grow with increasing magnetic field. The constant curvature of the data indicates that the correction to the Kondo splitting is given by  $c \ln(T_{K,0}/T_K)$ , where  $c$  is a constant; by comparing to the data we find  $c = 12$   $\mu$ eV.

We can also use these data to test predictions about the threshold field  $B_C$  necessary to split the Kondo peak. The existence of a threshold field is illustrated in Fig. 1(b). The peak does not start to split until  $B$  is greater than about 2.4 T. Figure 5(a) shows this threshold in more detail: at  $B = 2.0$  T the peak has not yet split, but by 2.4 T, the splitting is clearly evident. We can also extract information about  $B_C$  from data like those in Fig. 5. For a given magnetic field there is some Kondo temperature  $T_{K,C}$  for which this field is the critical field. For  $T_K$  below  $T_{K,C}$ , the Kondo peak is split and for  $T_K$  greater than  $T_{K,C}$  the peak is not split. This is illustrated by the data in Fig. 5(b) and in Fig. 5(c), which shows some individual traces from Fig. 5(b). In the middle of the valley, where the Kondo temperature

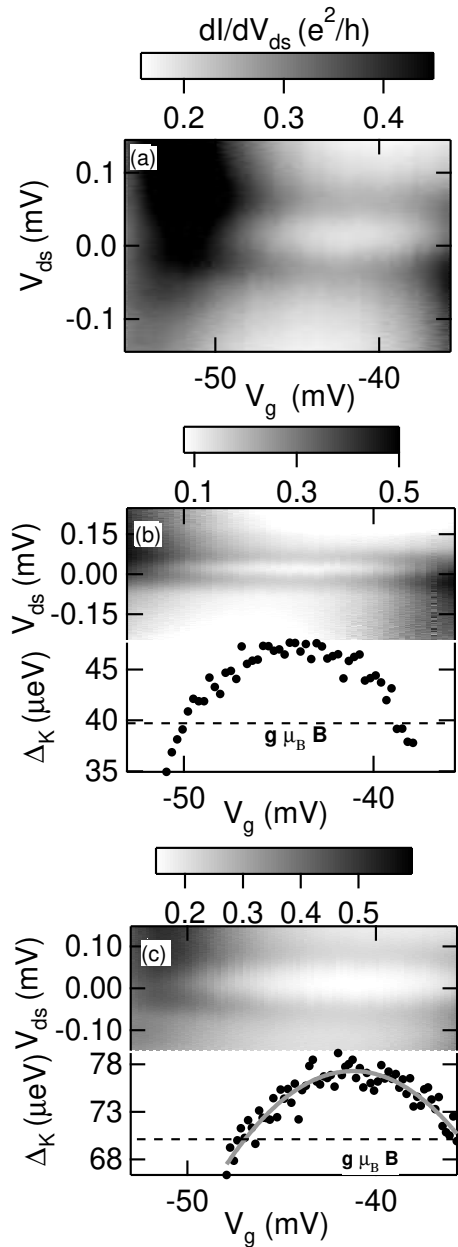


FIG. 3: (a) A Kondo feature with a magnetic field of 5 T applied. The Kondo peak at zero bias has clearly split into two peaks. One Coulomb charging peak is visible at  $-52$  mV; the other peak is not visible. (b) The top graph is the same as (a), but at  $B = 4.3$  T. The bottom graph shows  $\Delta_K$  as a function of  $V_g$ . The splitting is a maximum in the center of the valley, where the Kondo temperature is lowest. The dashed line indicates the Zeeman energy  $|g|\mu_B B$ . (c) Same as in (b) but at  $B = 7.5$  T. The gray line shows the result of fitting the data to a parabola. Note that in both (b) and (c) the splitting in the middle of the valley exceeds  $|g|\mu_B B$ .

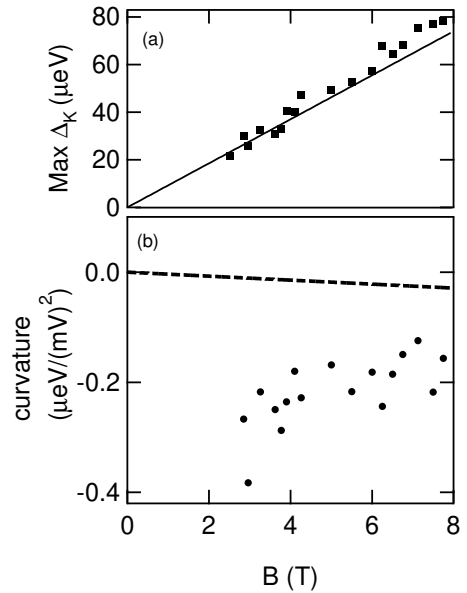


FIG. 4: (a) Splitting of the Kondo peak in the center of the Coulomb valley as a function of magnetic field. The solid line shows  $\Delta = |g|\mu_B B$  for  $|g| = 0.16$  determined by inelastic cotunneling. Above  $\sim 4$  T we find that  $\Delta_K > |g|\mu_B B$ . Below  $B = 2.4$  T no splitting is observed. (b) Curvature of  $\Delta_K$  vs  $V_g$  parabolas like those in Fig. 3(b)-(c). The prediction by Moore and Wen (dashed line) is that the curvature should decrease with field.

is lowest, the peak is clearly split. This splitting disappears toward the Coulomb charging peak where the Kondo temperature is higher. Because of the background from the Coulomb charging peak, it is difficult to reliably locate  $T_{K,C}$ . Instead, we identify a range of Kondo temperatures over which we are confident that the peak is split: this puts a lower bound on  $T_{K,C}$ .

To extract this bound, we locate the most negative gate voltage at which we still confidently observe the Kondo splitting. For the data in Fig. 5(b) and (c), this is at  $V_g = -49.9$  mV. To convert this to a Kondo temperature we use Equation (2). To find the center of the valley  $V_{g,0}$ , we use the location of the maximum of the fit of  $\Delta_K(V_g)$  to a parabola. We take into account the uncertainty in the determination of  $V_{g,0}$  to make the most conservative estimate of the lower bound. Knowing  $V_{g,0}$  we can convert  $V_g$  into a Kondo temperature using Equation (2). The lower bounds on  $T_{K,C}$  found in this way are shown as round dots in Fig. 5(d). At Kondo temperatures below these data points, the Kondo peak is split.

We can use our data to check predictions about  $T_{K,C}$ . Costi<sup>7</sup> predicts that  $B_C = 0.5T_0$ , where  $T_0$  is the half width at half-maximum of the Kondo resonance in the spectral function at  $T = 0$  and is related<sup>7,16</sup> to  $T_K$  by  $T_K = 0.433T_0$ . This prediction is shown as the solid line in Fig. 5(d): Costi predicts that below this line the Kondo peak should be split and above it the Kondo peak

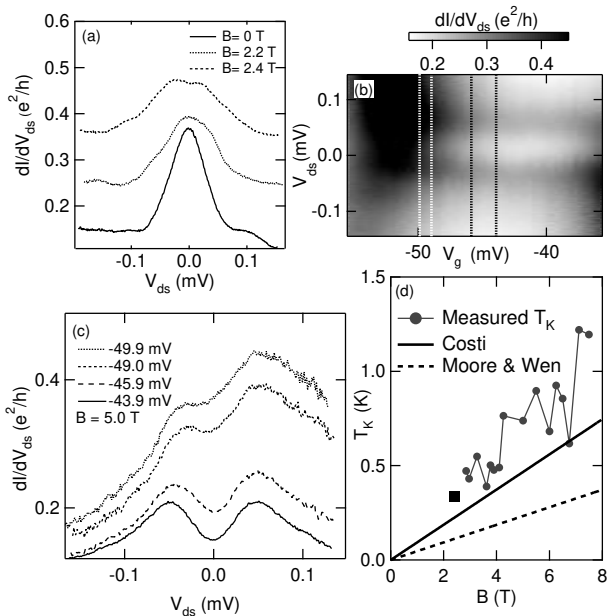


FIG. 5: (a) Drain-source sweeps in the middle of a Kondo valley at different magnetic fields. The onset of splitting is clear at  $B = 2.4$  T but not visible at 2.2 T. The curves have been offset by  $0.11 e^2/h$  for clarity. (b) Kondo valley with a 5 T field applied. The lines indicate the positions of the  $dI/dV_{ds}$  vs  $V_{ds}$  traces shown in (c). (c)  $dI/dV_{ds}$  vs  $V_{ds}$  at various gate voltages. In the center of the valley where  $T_K$  is a minimum the splitting is clear and symmetric. Closer to the charging peak the Kondo temperature is higher and the splitting is less pronounced, but still visible. (d) The dots mark the maximum  $T_K$  at which splitting is observed as a function of field. These data are extracted from data like those in (b) and (c) by measuring the gate voltage at which the splitting is barely visible. The conversion of this gate voltage to a Kondo temperature is explained in the text. The square data point marks the measurement of  $B_C$  from the data in (a). Predictions for  $B_C$  by Costi (solid line) and Moore and Wen (dashed line) are shown.

should not be split. However, this line lies below the

lower bound from our data indicating that at a given  $T_K$ ,  $B_C$  is smaller than predicted by theory. The dotted line in Fig. 5(d) is based on the work of Moore and Wen, who predict<sup>8</sup> the width and splitting of the spin-up component of the spectral function as a function of  $B/T_0$ . To model the Kondo peak arising from this spectral function we sum two lorentzians<sup>17</sup> with the width and splitting given by the predictions of Moore and Wen. We find that the splitting appears at  $B_C = T_0$ . This prediction is plotted as a dashed line in Fig. 5(d) and is clearly inconsistent with the data.

The observation that  $\Delta_K > \Delta$  by Kogan *et al.*<sup>11</sup> and Zumbühl *et al.*<sup>12</sup> demonstrates that we do not yet have a full theoretical understanding of the non-equilibrium Kondo effect. Our measurements of the Kondo temperature dependence of  $\Delta_K$  re-enforce this conclusion. While theory qualitatively describes the behavior of  $\Delta_K$  and  $B_C$  with  $T_K$ , it does not provide an accurate quantitative description. We find that  $\Delta_K$  decreases logarithmically with increasing  $T_K$ , but the prefactor of the logarithm is much larger than expected and is independent of  $B$ . There is clear evidence of a critical field  $B_C$  for the splitting of the Kondo peak. However, our data show that  $B_C$  is smaller than predicted by theory. Our results provide additional challenges to the theory of the non-equilibrium Kondo effect.

We thank D. Goldhaber-Gordon and D. Mahalu for designing and fabricating the SET devices used in this work and H. Shtrikman for growing the GaAs/AlGaAs heterostructures. We are grateful to J. Moore, T. Costi, L. Levitov, X.-G. Wen, W. Hofstetter, C. Marcus, D. Zumbühl, and J. Folk for discussions and to C. Cross, G. Granger, and K. MacLean for experimental help. This work was supported by the US Army Research Office under Contract DAAD19-01-1-0637, by the National Science Foundation under Grant No. DMR-0102153, and in part by the NSEC Program of the National Science Foundation under Award Number DMR-0117795 and the MR-SEC Program of the National Science Foundation under award number DMR 02-13282.

\* Electronic address: mkastner@mit.edu

† Current address: Department of Physics, University of Cincinnati, Cincinnati, OH 45221-0011

<sup>1</sup> L. I. Glazman and M. E. Raikh, JETP Lett. **47**, 452 (1988).

<sup>2</sup> T. K. Ng and P. A. Lee, Phys. Rev. Lett. **61**, 1768 (1988).

<sup>3</sup> D. Goldhaber-Gordon, H. Shtrikman, D. Mahalu, D. Abush-Magder, U. Meirav, and M. A. Kastner, Nature (London) **391**, 156 (1998).

<sup>4</sup> S. M. Cronenwett, T. H. Oosterkamp, and L. P. Kouwenhoven, Science **281**, 540 (1998).

<sup>5</sup> D. Goldhaber-Gordon, J. Göres, M. A. Kastner, H. Shtrikman, D. Mahalu, and U. Meirav, Phys. Rev. Lett. **81**, 5225 (1998).

<sup>6</sup> Y. Meir, N. S. Wingreen, and P. A. Lee, Phys. Rev. Lett.

**70**, 2601 (1993).

<sup>7</sup> T. A. Costi, Phys. Rev. Lett. **85**, 1504 (2000).

<sup>8</sup> J. E. Moore and X.-G. Wen, Phys. Rev. Lett. **85**, 1722 (2000).

<sup>9</sup> A. Rosch, J. Paaske, J. Kroha, and P. Wölfle, Phys. Rev. Lett. **90**, 076804 (2003).

<sup>10</sup> A. Rosch, T. A. Costi, J. Paaske, and P. Wölfle, Phys. Rev. B **68**, 014430 (2003).

<sup>11</sup> A. Kogan, S. Amasha, D. Goldhaber-Gordon, G. Granger, M. A. Kastner, and H. Shtrikman, Phys. Rev. Lett. **93**, 166602 (2004).

<sup>12</sup> D. M. Zumbühl, C. M. Marcus, M. P. Hanson, and A. C. Gossard (2004), cond-mat/0408276.

<sup>13</sup> F. D. M. Haldane, Phys. Rev. Lett. **40**, 416 (1978).

<sup>14</sup> T. A. Costi, A. C. Hewson, and V. Zlatić, *J. Phys.: Condens. Matter* **6**, 2519 (1994).

<sup>15</sup> N. S. Wingreen and Y. Meir, *Phys. Rev. B* **49**, 11040 (1994).

<sup>16</sup> T. A. Costi (private communication).

<sup>17</sup> J. E. Moore (private communication).